

Spin-lattice coupling, frustration and magnetic order in multiferroic RMnO_3 X. Fabreges¹, S. Petit¹, I. Mirebeau¹, S. Pailhes¹, L. Pinsard², A. Forget³, M. T. Fernandez-Diaz⁴ and F. Porcher¹¹ Laboratoire Leon Brillouin, CEA-CNRS, CE-Saclay, 91191 Gif-sur-Yvette, France² Laboratoire de Physico-Chimie de l'Etat Solide, ICM MO, Université Paris-Sud, 91405 Orsay, France³ Service de Physique de l'Etat Condense, CEA-CNRS, CE-Saclay, 91191 Gif-sur-Yvette, France and⁴ Institut Laue Langevin, 6 rue Jules Horowitz, BP 156X, 38042 Grenoble France.

(Dated: 01/03/2009)

We have performed high resolution neutron diffraction and inelastic neutron scattering experiments in the frustrated multiferroic hexagonal compounds RMnO_3 ($R = \text{Ho}, \text{Yb}, \text{Sc}, \text{Y}$), which provide evidence of a strong magneto-elastic coupling in the whole family. We can correlate the atomic positions, the type of magnetic structure and the nature of the spin waves whatever the R ion and temperature. The key parameter is the position of the Mn ions in the unit cell with respect to a critical threshold of $1/3$, which determines the sign of the coupling between Mn triangular planes.

Multiferroics have aroused a great attention for the last years, as the coupling between ferroelectric and magnetic orderings in these materials may open the route to novel promising electronic devices. Magnetic frustration combined with a striking magneto-elastic coupling seems to be at the origin of their properties, a cocktail that has a strong potential for novel physics [1]. These compounds are however rare, and far from being fully understood. Indeed, ferroelectricity imposes a non centrosymmetric space group [2], while magnetic frustration favors complex magnetic orders [3, 4].

The RMnO_3 compounds, where R is a rare earth ion, follow these conditions. In orthorhombic RMnO_3 , ($R = \text{Eu}, \text{Gd}, \text{Tb}, \text{Dy}$), where the strong GdFeO_3 -type distortion lifts the orbital degeneracy, magnetic frustration arises from competing super-exchange interactions [5], yielding incommensurate magnetic structures [6]. This peculiar ordering suggested a novel coupling between dielectric and magnetic collective modes [7]. In hexagonal RMnO_3 with smaller R ionic radius, ($R = \text{Ho}, \text{Er}, \text{Yb}, \text{Lu}, \text{Y}$), magnetic frustration arises from the triangular geometry [8], yielding 120° Neel orders for the Mn moments [9]. In YMnO_3 and LuMnO_3 , where Y and Lu are non magnetic, an iso-structural transition was recently observed at the Neel temperature T_N [10], namely each ion "moves" inside the unit cell when Mn moments get ordered. This effect provided evidence for a giant magneto-elastic coupling, likely connected with an increase of the ferroelectric polarization [11]. Its origin remains unexplained so far.

To shed light on these materials, we carried out high resolution neutron diffraction and inelastic neutron scattering in four RMnO_3 ($R = \text{Y}, \text{Sc}, \text{Ho}, \text{Yb}$), with either non magnetic (Y, Sc) or magnetic (Ho, Yb) R ion, showing (Ho, Sc) or not (Y, Yb) a spin reorientation at T_{SR} with temperature [12, 13, 14]. We show that the iso-structural transition is a systematic feature in the hexagonal series. In addition, we establish a correlation between the atomic positions, the type of magnetic structure, and the nature of the spin waves, whatever the com-

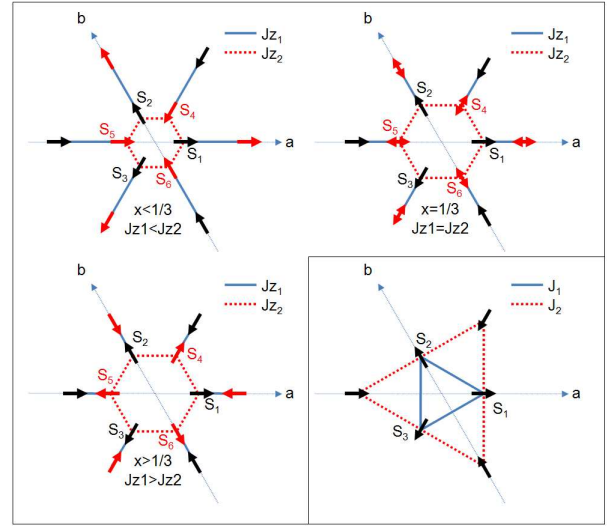


FIG. 1: [Colors on line]. Sketch of the hexagonal MnO planes with out-of-plane exchange paths J_{z1} (between S_4 and S_3) and J_{z2} (between S_4 and S_1 as well as S_4 and S_2). Black (red) arrows depict the positions of the Mn spins within $z=0$ ($z=1/2$) Mn planes. S_1, S_2 and S_3 are located at $(x; 0; 0)$, $(0; x; 0)$, $(-x; -x; 0)$, while S_4, S_5, S_6 at $(x; x; 1/2)$, $(1-x; 0; 1/2)$ and $(0; 1-x; 1/2)$. Double arrows are used when several spin orientations can be stabilized. Inset: sketch of the hexagonal MnO plane with in-plane exchange paths J_1 and J_2 .

pound and its magnetic structure. We show that the key parameter is the position x of the Mn ions within the triangular plane with respect to a critical threshold of $1/3$ which tunes the sign of the interplane exchange interaction. We justify this result by simple energy arguments. Thanks to the magneto-elastic coupling, the atomic motion helps releasing the frustration by selecting a given magnetic structure, depending on the x value. This process recalls the spin-Peierls states stabilized in several geometrically frustrated 2D or 3D compounds [15, 16].

Hexagonal RMnO_3 compounds consist of stacked Mn-O and R layers, the Mn ions forming a nearly ideal two dimensional triangular lattice [17]. They crystallize in the $P6_3cm$ space group, with two Mn-O planes per unit cell. As shown on Figure 1, Mn coordinates depend on a unique parameter x . For $x \neq 1/3$, two different exchange paths J_1 and J_2 can be defined between Mn moments in a given Mn plane (inset Fig. 1). The triangular symmetry and hence the geometrical frustration within a Mn plane is however preserved whatever the x value. The Mn-Mn interactions between adjacent Mn planes are due to super-super exchange paths, via the apical oxygen ions of MnO_5 bipyramids. These interactions lead to a 3D magnetic ordering below T_N . Again, as soon as $x \neq 1/3$, two different paths, and thus two different interactions, J_{z1} and J_{z2} , can be distinguished (Fig. 1), while for $x = 1/3$ all paths become equivalent. The value $x = 1/3$ is therefore a critical threshold which determines the sign of the effective interplane exchange $J_{z1} - J_{z2}$ (the same sign as that of $x - 1/3$). As shown below, this quantity determines in turn the stability of the magnetic phases and the nature of the spin waves.

Whatever the x value and the R magnetism, the Mn magnetic moments order in 120° arrangements, with four different possible structures (inset Fig. 2), labeled from the irreducible representations (IR) Γ_i , $i = 1-4$ of the $P6_3cm$ space group with $k = 0$ propagation vector [12, 18]. For Γ_1 and Γ_4 , Mn moments are perpendicular to a and b axes, and their arrangement in the $z = 1/2$ plane are either antiparallel (Γ_1) or parallel (Γ_4) with respect to $z = 0$. The same picture holds for Γ_2 and Γ_3 with spins along a and b axes.

High-resolution neutron powder diffraction patterns were collected versus temperature on the D2B and 3T2 instruments, at ILL and LLB-Orphee reactors respectively. Powder samples HoMnO_3 , ScMnO_3 and YbMnO_3 were prepared as described in [19] and characterized by x-ray diffraction. Data were analyzed using the Fullprof and Basireps softwares [20, 21], allowing us to determine the atomic positions and the magnetic structures versus temperature precisely. The magnetic structures and transition temperatures agree with previous determinations [9, 12]. It is worth noting that HoMnO_3 and ScMnO_3 undergo a second magnetic transition at T_{SR} corresponding to the reorientation of the Mn spins.

Figure 2 shows the temperature dependence of the Mn position x for the three samples. As a striking feature, in HoMnO_3 , x exhibits an unprecedented large change (of about 3%), which occurs at T_N , providing evidence for an iso-structural transition concomitant with the magnetic ordering. Smaller changes occur at T_N in ScMnO_3 and YbMnO_3 . These results confirm those previously obtained [10] in Y and LuMnO_3 , and show that this transition is universal in the hexagonal RMnO_3 series. As noticed in Ref. 10, the variations of x versus T depend of the rare-earth ion, namely x increases below T_N in Ho

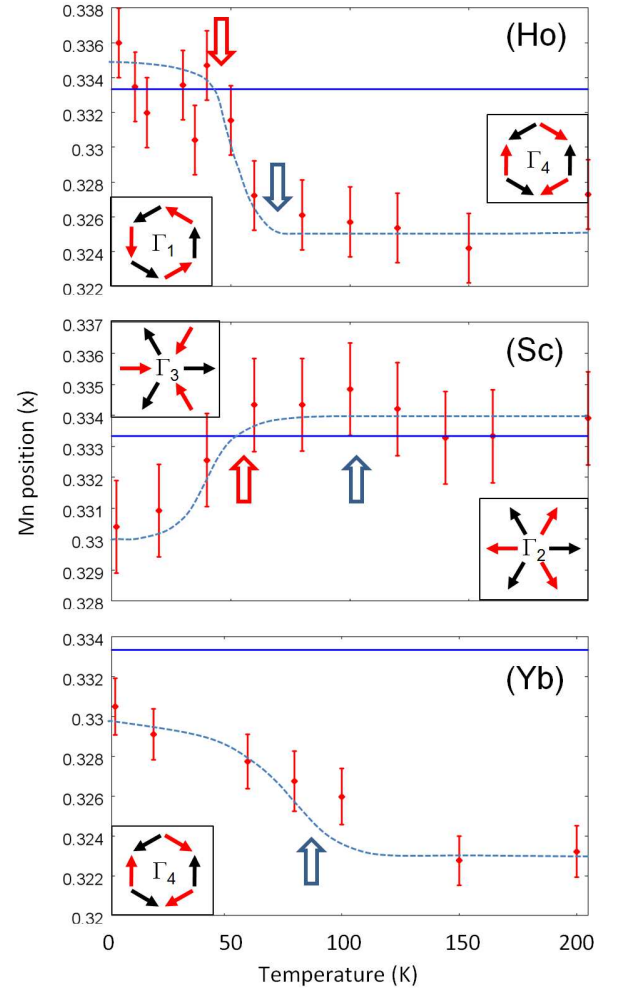


FIG. 2: [Color online]. Refined Mn positions in the unit cell obtained from high-resolution neutron powder diffraction. Blue and red arrows indicate respectively the Neel and the spin reorientation temperatures. Lines are guides to the eyes. Right insets: Mn magnetic configuration for $T_{SR} < T < T_N$. Left insets: Mn magnetic configuration $T < T_{SR}$.

and YbMnO_3 , whereas it decreases in ScMnO_3 . Moreover, we also discern important changes at the reorientation transition. In HoMnO_3 , x increases with decreasing temperature and crosses the $1/3$ threshold exactly at the spin reorientation temperature (T_{SR}). The reverse situation holds for ScMnO_3 , where x decreases upon cooling, becoming lower than $1/3$ at T_{SR} . Finally, in YbMnO_3 , which shows no reorientation transition, x increases at T_N but remains lower than $1/3$ in the whole temperature range.

All these features can be explained by considering the strategic position of the Mn ions. We argue that x is the key parameter that controls the sign of $J_{z1} - J_{z2}$ and thus drives the magnetic ordering. Namely for $x > 1/3$, the exchange path along J_{z1} is longer than along J_{z2} and we expect $J_{z1} - J_{z2} < 0$. The reverse situation

R ion	IR		Positions	
	T _N	1.5K	T _N	1.5K
Yb	4	4	0.3270 (15)	0.3310 (14)
Ho	4	1	0.3261 (21)	0.3359 (19)
Sc	2	3	0.3342 (18)	0.3304 (17)
Y	1	1	0.3330 (17)	0.3423 (13)

TABLE I: Mn position in RMnO₃ compounds correlated with their magnetic structures defined by irreducible representations. YMnO₃ positions are taken from Ref. 10

occurs for $x = 1/3$. A careful look at the positions and magnetic structures summarized in table I shows that $x = 1/3$ is associated with Γ_3 and Γ_4 while $x = 2/3$ corresponds to Γ_1 and Γ_2 . This scheme also explains the occurrence of a spin reorientation transition when x crosses the 1/3 threshold. In this case, $J_{z1} - J_{z2}$ changes sign, resulting in a change from Γ_1 towards Γ_4 (Ho) or from Γ_2 towards Γ_3 (Sc). The crucial importance of the $J_{z1} - J_{z2}$ coupling can be further justified by calculating the magnetic energy E (per unit cell) of the Mn moments in a mean field approximation. E is readily obtained by writing the Heisenberg Hamiltonian: $H = H_p + H_z$, with $H_p = \sum_{\langle p,j \rangle} J_{S_i S_j}$, and $H_z = \sum_j J_z S_i S_j$, where the sums run over nearest neighbors and the subscripts p and z refer to in plane and out of plane interactions respectively. Because of the triangular arrangement, we have $\sum_{i=1,2,3} S_i = \sum_{i=4,5,6} S_i = 0$, which in turn implies: $E = \frac{3}{2} J S^2 + (J_{z1} - J_{z2}) (S_3 S_4)$. Depending on its sign, parallel or antiparallel orientations of S_3 and S_4 are expected, giving rise to the four magnetic structures described above. Within this simple picture, Γ_1 and Γ_2 IR minimize the energy for $J_{z1} - J_{z2} > 0$ while Γ_3 and Γ_4 are favored for $J_{z1} - J_{z2} < 0$. This is in exact agreement with the results summarized in Table I.

A straightforward way to confirm our explanation is to determine the value of $J_{z1} - J_{z2}$ by an independent measurement. This can be easily done by measuring the spin wave dispersion along the c -axis. For this purpose we carried out inelastic neutron scattering experiments on the cold triple-axis 4F spectrometer installed at LLB-Orphee, on large single crystals of YMnO₃, YbMnO₃ and HoMnO₃ grown by the floating zone technique.

Figure 3(left) shows a color map of the dynamical structure factor measured as a function of energy and wavevector in YMnO₃, YbMnO₃ and HoMnO₃. These maps were obtained by collecting energy scans taken at different $(1;0;Q)$ wavevectors. The measurements were performed at 2 K in the first two cases, and at two temperatures just above and below the re-orientation temperature T_{SR} for HoMnO₃. Different features can be seen from these experimental data, including crystal field levels (Yb and Ho). A comprehensive investigation of these features is however beyond the scope of this paper and we would like to focus on the low energy spin wave excitations labelled with arrows. We notice that

in YMnO₃ and YbMnO₃, this particular branch displays upwards (Yb) or downwards (Y) dispersions, revealing opposite couplings along c . Similarly in HoMnO₃, when crossing the reorientation T_{SR} , the curvature changes from upwards to downwards, indicating a reversal of the magnetic interaction along the c -axis.

To get a quantitative information about these couplings, we performed a spin wave analysis of the Heisenberg Hamiltonian $H = H_p + H_z$ defined above, taking into account additional planar and uniaxial anisotropy terms [22, 26]. Figure 3(right) shows the dynamical structure factors calculated on the basis of this model as a function of energy transfer $\hbar\omega$ and wavevector $(1;0;Q)$. In this approach, six spin wave modes are expected. Along c , four of them are almost degenerate. They exhibit a large gap due to the planar anisotropy, as well as a very weak dispersion. On Figure 3 (right), these modes correspond to the flat branch sitting at 5 meV (Ho,Y) or 6 meV (Yb). The two remaining modes correspond to the Goldstone modes of the magnetic structure. In $q = 0$ limit, they can be seen as global rotations of the 120 pattern inside the basal planes. They couple via the J_z interactions, resulting in either in phase or out of phase rotations. These two modes are pointed out by arrows in Figure 3 (right). Actually, one of them has a vanishing intensity but can still be observed around (101). Assuming antiferromagnetic couplings J_{z1} and J_{z2} , we can determine from the data $J_{z1} - J_{z2} = 0.0050(5)$ meV in YMnO₃ and $J_{z1} - J_{z2} = 0.012(2)$ meV in YbMnO₃. For HoMnO₃, the neutron data are well modelled with $J_{z1} - J_{z2} = 0.0038(5)$ meV at $T = 45$ K T_{SR} and with $J_{z1} - J_{z2} = 0.0018(5)$ meV at $T = 27$ K T_{SR} . We note that the corresponding signs of $J_{z1} - J_{z2}$ deduced from these measurements are fully consistent with the diffraction analysis.

Our analysis emphasizes the double origin of the magnetic frustration. The Mn triangular planes are geometrically frustrated for antiferromagnetic interactions. In addition, adjacent Mn planes are coupled along the c axis by self-competing interactions. The Mn shift with respect to the 1/3 position does not suppress the rotational invariance in the Mn plane, but clearly lifts the interplane frustration, allowing 3D ordering. Depending on x , either $(\Gamma_1; \Gamma_2)$ or $(\Gamma_3; \Gamma_4)$ structures are stabilized. The remaining degree of freedom in the system is the global rotation of a 120 Neel order around the c -axis. Namely, to stabilize Γ_1 or Γ_2 (Γ_3 or Γ_4), the Mn magnetic moments must couple to the (a;b) crystal axes.

On the one hand, residual anisotropic interactions among Mn ions can in principle select a given orientation in a Mn plane. As revealed by the exceptionally small uniaxial gap observed in YMnO₃ [22, 26], these interactions are weak. They are not sufficient to break the triangular symmetry, so that two-dimensional spin liquid fluctuations remain [22]. On the other hand, one could argue that R-Mn interactions (when R is magnetic) play

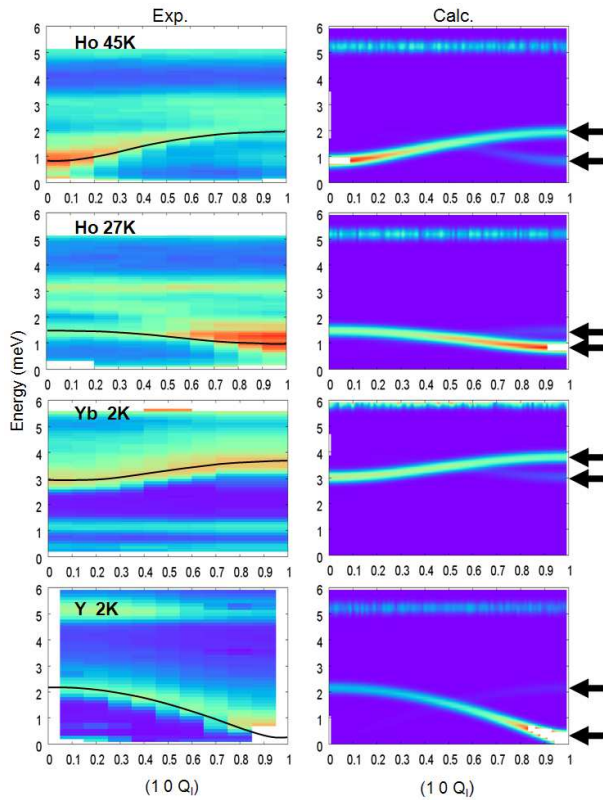


FIG. 3: (color online.) Maps of the dynamical structure factor in Ho, Yb and Y MnO₃. The neutron intensity is plotted versus the energy transfer $\hbar\omega$ and wave vector $(1;0;Q_x)$. Left panel: experimental results from inelastic neutron scattering. Black lines highlight the low energy spin wave modes. Additional Q_x -independent lines in Yb and Ho MnO₃ maps are due to crystal field excitations. Right panel: spin wave dispersion curves calculated using an Heisenberg Hamiltonian. Black arrows indicate the two Goldstone modes (see text).

a significant role. Indeed, the R moments on the 4b site order at T_N in the Mn molecular field, while their orientations are clearly coupled to the Mn ones, through an energy term of anisotropic nature [14]. Our spin wave measurements (Fig 3) show that the uniaxial anisotropy gap in Yb MnO₃ (3 meV) varies with temperature like the Yb moment, providing evidence for such R-Mn coupling. Nevertheless, we shall not conclude that the Mn orientation in the (a;b) plane is completely determined by this interaction. For instance, spin reorientation transitions of the Mn sublattice may occur (Sc, Ho) or not (Y, Yb) whatever the R magnetism.

In conclusion, our elastic and inelastic neutron scatter-

ing experiments clearly show the crucial role of the Mn position in determining both the magnetic structure and the spin wave modes. The onset of Mn magnetic orderings at T_N or T_{SR} correlates with the Mn position. The magnetic orders and spin excitations in the whole series result from a subtle interplay of magneto-elastic coupling, frustrated intra- and inter-plane Mn-Mn interactions and R-Mn interactions. The strong importance of inter-plane interactions strongly suggests that the shift of the Mn position, which releases the frustration along the c axis, is a key ingredient at the origin of the multiferroicity in the hexagonal RMnO₃ family. We thank E. Suard for her help in the D2B experiment and V. Simonet and F. Damay-Rowe for useful discussions.

-
- [1] S-W Cheong, M. Mostovoy, Nature Materials 6, 13 (2007).
 - [2] M. Fiebig, J. Phys. D: Appl. Phys. 38, R 123 (2005).
 - [3] J. E. Greedan J. Mater. Chem. 11, 37 (2001).
 - [4] R. Moosner and A. P. Ramirez Physics Today 59, 24 (2006).
 - [5] T. Kikkawa et al, Phys. Rev. B 68, 060403(R) (2003).
 - [6] M. Kenzelmann et al. Phys. Rev. Lett. 95, 087206 (2005).
 - [7] H. Katsura, A. V. Balatsky and N. Nagaosa Phys. Rev. Lett. 98, 027203 (2007).
 - [8] Th. Jolicoeur, J. C. Le Guillou, Phys. Rev. B 40, 2727 (1989).
 - [9] A. Muñoz et al, Chem. Mater., 13, 1497-1505 (2001).
 - [10] S. Lee et al. Nature 451, 805 (2008).
 - [11] S. Lee et al. Phys. Rev. B 71 180413(R) (2005)
 - [12] A. Muñoz et al, Phys. Rev. B, 62, 9498 (2000).
 - [13] P. J. Brown and T. Chatterji, J. Phys. Cond. Matter, 18, 10085-10096 (2006).
 - [14] X. Fabreges et al. Phys. Rev. B, 78, 214422 (2008).
 - [15] F. Becca and F. Mila Phys. Rev. Lett., 89, 037204 (2002).
 - [16] O. Tchernyshyov, R. Moosner and S. L. Sondhi Phys. Rev. Lett., 88, 067203 (2002).
 - [17] T. Katsufuji et al, Phys. Rev. B 66, 134434 (2002).
 - [18] E. F. Bertaut, C. R. A. S. 252, 76 (1961).
 - [19] J. A. Alonso, M. J. Martínez-Lope, M. T. Casais, M. T. Fernández-Díaz, Inorg. Chemistry, 39, 917-923 (2000).
 - [20] J. Rodríguez-Carvajal, Physica B, 192, 55-69 (1993)
 - [21] J. Rodríguez-Carvajal, <http://www.jillieu/sites/fullprof/php/program>
 - [22] T. J. Sato et al, Phys. Rev. B 68, 014432 (2003).
 - [23] J. Park et al. Phys. Rev. B 68, 104426 (2003).
 - [24] O. P. Vajk, M. Kenzelmann, J. W. Lynn, S. B. Kim, S.-W. Cheong, Phys. Rev. Lett. 94, 087601 (2005).
 - [25] T. Chatterji, S. Ghosh, A. Singh, L. P. Regnault and M. Rheinstadter, Phys. Rev. B 76, 144406 (2007).
 - [26] S. Petit et al, Phys. Rev. Lett. 99, 266604 (2007).
 - [27] S. Pailhes et al, Phys. Rev. B 79, 134409 (2009).